ELSEVIER

Energy and Buildings 28 (1998) 219–227

ENERGY AND BUILDINGS

Calculation of convective heat transfer coefficients of room surfaces for natural convection

Hazim B. Awbi *

Department of Construction Management and Engineering, The University of Reading, Reading, UK

Received 3 July 1997; accepted 12 March 1998

Abstract

Convective heat transfer from internal room surfaces has major effect on the thermal comfort, air movement and heating and cooling loads for the room. Recent studies have shown that the values of convective heat transfer coefficient used in building thermal models greatly influence the prediction of the thermal environment and energy consumption in buildings. In computational fluid dynamics (CFD) codes for room air movement prediction, accurate boundary conditions are also necessary for a reliable prediction of the air flow. However, most CFD codes use 'wall functions' derived from data relating to the flow in pipes and flat plates which may not be applicable to room surfaces. This paper presents results for natural convection heat transfer coefficients of a heated wall, a heated floor and a heated ceiling which have been calculated using CFD. Two turbulence models have been used to calculate these coefficients: a standard $k-\varepsilon$ model using 'wall functions' and a low Reynolds number $k-\varepsilon$ model. The computed results are compared with data obtained from two test chambers.

Keywords: Residential buildings; Commercial buildings; Heat transfer; Computational fluid dynamics; Simulation; Laboratory

1. Introduction

The representation of the thermal boundary conditions of a room surface has a major influence on the accuracy of predicting the thermal comfort and heating and cooling loads for the room specially where large glazed surfaces are present. Recent studies have partly attributed the large discrepancies which exist between widely used building thermal models to the difference between the heat transfer coefficients used in these models, e.g., Ref. [1]. A recent paper [2] has also shown the existence, in the literature, of a large variation in the values of convective heat transfer coefficients (h) for room surfaces.

Computational fluid dynamics (CFD) is being extensively used in room air movement research and for the performance assessment of air distribution systems in buildings. The boundary conditions which are used for representing the heat and momentum transport from internal room surfaces have a profound influence on the accuracy of predicting the heat transfer from these surfaces and the air movement within the room. In some situations, the flow is dominated by natural convection but in others, particularly when mechanical ventilation is present, a mixed flow (i.e., natural/forced convection) could be present

Most research and commercial CFD codes use 'logarithmic wall functions' to describe the momentum and heat transfer from the internal surfaces of a room. The majority of these wall functions have been empirically derived for forced convection in pipes and flat plates [3]. However, the flow over most internal room surfaces is either produced by natural convection or by an air jet. For a plane wall jet the wall function for momentum deviates from that for a boundary layer flow when $y^+ > 130$, i.e., in the outer region of the jet [4]. Niu and van der Kooi [5] have shown that when using wall functions with a standard $k-\varepsilon$ turbulence model in a CFD code, the heat transfer from a window is greatly influenced by the position of the first grid point from the surface, i.e., the value of $y_p{}^+$. This is also confirmed in this paper as will be shown later.

Henkes and Hoogendroon [6] tested various turbulence models for the calculation of natural convection heat transfer from a vertical heated plate. The models they examined can be grouped as: (i) a standard $k-\varepsilon$ model; (ii) low Reynolds number $k-\varepsilon$ models; and (iii) an algebraic stress model. They found that the Cebeci–Smith algebraic model calculates a low heat transfer coefficient whereas the standard $k-\varepsilon$ model gives a high value compared with experimental data.

* Corresponding author. Tel.: +44 118 9316786; fax: +44 118 9313856; e-mail: h.b.awbi@rdg.ac.uk

0378-7788/98/$ - see front matter
PII S0378-7788(98)00022-X

They, therefore, concluded that the accurate prediction of surface heat transfer requires the use of a low Reynolds number $k-\varepsilon$ model. In particular they found that the models of Lam and Bremhorst, Chien and Jones and Launder performed best up to a Grashof number of 10^{11}.

The heat transfer from horizontal heated surfaces, such as the floor and ceiling, has not been studied to the same extent as a vertical surface and data for such surfaces is rather scant. The heat transfer from these surfaces is quite different from a vertical surface. These surfaces are of practical interest when, for example, a floor heating system is used or when thermal stratification caused by a heated ceiling is studied.

In this paper, two methods have been used to calculate the value of h from the heated surfaces of a two-dimensional cavity under natural convection. A standard $k-\varepsilon$ turbulence model with 'wall function' expressions and the low Reynolds number $k-\varepsilon$ model of Lam and Bremhorst [7] have been used. In both cases the VORTEX (ventilation of rooms with turbulence and energy exchange) program [8] has been used in the calculation. The calculated results are compared with experimental data obtained from measurements in two test chambers for a Grashof number range of 9×10^{8}–1×10^{11}.

2. Theoretical analysis and governing equations

2.1. Momentum transport near the wall region

The transport equation for a two-dimensional turbulent boundary layer with zero pressure gradient is:

$$u\frac{\partial u}{\partial x}+v\frac{\partial u}{\partial y}=\frac{1}{\rho}\frac{\partial \tau}{\partial y} \tag{1}$$

where the total shear stress, τ, is given by:

$$\tau=\tau_l+\tau_t=\mu\frac{\partial u}{\partial y}=\rho\overline{u'v'} \tag{2}$$

The first term on the right hand side of Eq. (2) represents the fluid (laminar) shear stress, τ_l, and the second term represents the Reynolds (turbulent) shear stress, τ_t.

Fig. 1 represents the variation in the ratio τ_t/τ with y^+ and it can be seen that as the wall is approached τ_t decreases. In the figure, $u_\tau=\sqrt{\tau_w/\rho}$ is the friction velocity, where τ_w is the shear stress at the wall, i.e., at $y=0$. The figure shows that at $y^+=11.6$, $\tau_t\cong\tau_l$ and for $y^+=30$, $\tau_t\cong0.9\tau_w$.

The variation of u^+ with y^+ for a boundary layer and a plane wall jet is shown in Fig. 2. Four regions may be identified according to the value of y^+. The viscous sublayer region is given by $y^+<8$; which is then followed by the transition region (buffer zone) which is represented by $8<y^+<40$; the turbulent inner region (log-law zone) which is represented by $40<y^+<130$; and the outer region which is given by $y^+>130$. It should be noted that the flow in a plane jet is similar to a boundary layer flow up to $y^+\approx130$ but is different for greater values. This would suggest differences in heat convection between a surface which is covered by a wall jet from that which is covered by a boundary layer.

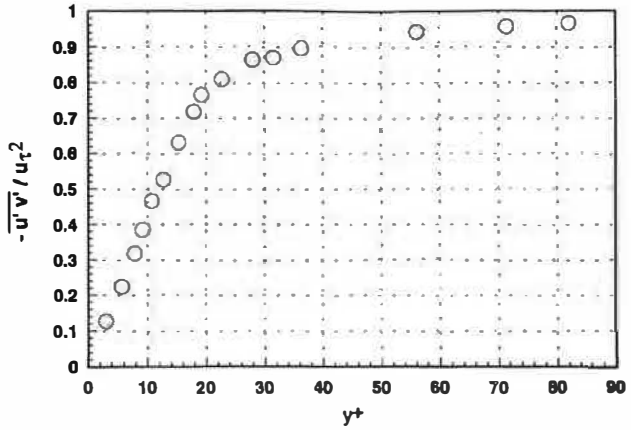

Fig. 1. Dimensionless Reynolds shear stress distribution in a wall boundary layer [9].

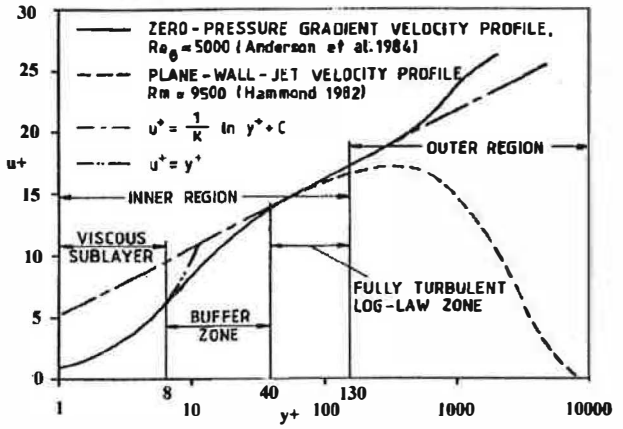

Fig. 2. Non-dimensional velocity profile in a turbulent boundary layer and a plane wall jet [10].

2.2. Turbulence model

The transport equations for the kinetic energy (k) and the dissipation rate (ε) of turbulence energy for 2D flow are given by [7]:

$$u\frac{\partial k}{\partial x}+v\frac{\partial k}{\partial y}=\frac{\partial}{\partial y}\left[\left(\nu+\frac{\nu_t}{\sigma_k}\right)\frac{\partial k}{\partial y}\right]+P_k-\varepsilon+D \tag{3}$$

$$u\frac{\partial \varepsilon}{\partial x}+v\frac{\partial \varepsilon}{\partial y}=\frac{\partial}{\partial y}\left[\left(\nu+\frac{\nu_t}{\sigma_\varepsilon}\right)\frac{\partial \varepsilon}{\partial y}\right]+(C_{\varepsilon1}f_1P_k-C_{\varepsilon2}f_2)\frac{\varepsilon}{k}+E \tag{4}$$

where

$$P_k=\nu_t\left(\frac{\partial u}{\partial y}\right)^2 \tag{5}$$

$$\nu_t=C_\mu f_\mu k^2/\varepsilon \tag{6}$$

D and E are additional terms which are sometimes included to improve the representation of the near-wall behaviour in the case of low Reynolds number models; the f's are functions for modifying the C_ε constants in the case of low Reynolds number models.

The f-functions used in the Lam and Bremhorst model are given by:

$$f_\mu=(1-e^{-A_\mu R_k})^2\left[1+\frac{A_t}{R_t}\right] \quad (7)$$

$$f_1=1+\left[\frac{A_{C1}}{f_\mu}\right]^3 \quad (8)$$

$$f_2=1-e^{-R_t^2} \quad (9)$$

where

$$R_t=k^2/(\nu\varepsilon) \quad (10)$$

$$R_k=\sqrt{k}y/\nu \quad (11)$$

Table 1 gives values of the constants used in the standard and low Reynolds number turbulence models [7].

2.3. Heat transfer near the wall region

As the velocity field close to the wall depends on the rate of transport of momentum to the surface (τ_w), the temperature field depends on the rate of heat transfer from the surface to the fluid (q_w). Representing the 'friction temperature' by:

$$T_\tau=\frac{q_w}{\rho C_p u_\tau} \quad (12)$$

a dimensionless temperature, T^+, can be defined as follows:

$$T^+=\frac{T_w-T}{T_\tau} \quad (13)$$

where T_w is the surface temperature.

2.4. Wall boundary conditions

Boundary values for *all* the dependent variables to be solved must be specified and used in the solution of the field equations. The standard $k-\varepsilon$ model is only valid in regions of the flow where the Reynolds number is high. However, the Reynolds number is always low at the wall for non-slip conditions.

At the wall, non-slip conditions are specified for the velocity, and the kinetic energy of turbulence and its dissipation rate are as follows:

$$k_w=0 \text{ and } (\partial\varepsilon/\partial y)_w=0$$

i.e., ε reaches a constant value at the wall. Hence, the kinetic energy dissipation at the first computational point from a surface, ε_p, will be dependent upon the location of the point within the boundary layer. If it is located outside the viscous sublayer, such as when a standard $k-\varepsilon$ model is used, then the value of ε_p is expressed by:

Table 1
Constants for $k-\varepsilon$ turbulence models

D	E	C_μ	$C_{\varepsilon 1}$	$C_{\varepsilon 2}$	σ_k	σ_ε	A_μ	A_t	A_{C1}
0	0	0.09	1.44	1.92	1.0	1.3	0.0165	20.5	0.05

$$\varepsilon_p=C_\mu^{0.75}k_p^{}/(\kappa y_p) \quad (14)$$

The value of k at that point (k_p) is obtained by solving the conservation equation for k assuming that $k_w=0$.

If the first computational point is located within the viscous sublayer zone, such as when a low Reynolds number model is used, then ε_p should have a value >0. Chen [11] found that the expression below for ε_p achieves a converged solution:

$$\varepsilon_p=2\nu_l k/y_p^2 \quad (15)$$

Eqs. (14) and (15) have been used for calculations in this paper.

It can be deduced, therefore, that the distance from the wall at which the boundary values are specified will depend on the type of turbulence model used in the calculations. In general, the first point from the wall should be located within the turbulent zone (logarithmic region) when a standard $k-\varepsilon$ model with wall functions is used, and in the viscous sublayer zone when a low Reynolds number model is used. The analysis pertaining to these two regions is presented below.

2.4.1. Turbulent inner region (standard $k-\varepsilon$ model)

In this region, τ_l is small compared with τ_t and may be neglected. This is true for $y^+>30$, as shown in Fig. 1.

Ignoring the laminar shear stress, Eq. (2) reduces to:

$$\tau_t/\rho=-\bar{u}'\bar{v}'=u_\tau^2 \quad (16)$$

Using Eq. (15) and the mixing length expression:

$$\frac{\partial u}{\partial y}=\frac{u_\tau}{\kappa y} \quad (17)$$

the logarithmic expression below is obtained, e.g., see Ref. [12]:

$$u^+=1/\kappa \ln y^+ + C \quad (18)$$

where κ is the Karman constant and C is a constant which ranges in value between 4.9 to 5.6.

The heat transfer in the turbulent boundary layer is mainly by convection and the heat diffusion may be ignored. Using the Reynolds analogy between heat and momentum transfer, a similar expression can be obtained for the dimensionless temperature, T^+, viz:

$$T^+=1/\kappa_h \ln y^+ + C_h \quad (19)$$

where κ_h is the Karman constant for heat transfer $\cong 0.44$ and

C_h is a function of the laminar and turbulent Prandtl numbers, σ and σ_t. Usually, C_h is expressed as a function of σ and σ_t, viz:

$$C_h=f(\sigma/\sigma_t)$$

A widely used expression for C_h is that due to Jayatilaka [12], i.e.,

$$f(\sigma/\sigma_t)=9.24\{(\sigma/\sigma_t)^{3/4}-1\} \times\{1+0.28\exp(-0.007\sigma/\sigma_t)\} \quad (20)$$

Eqs. (18) and (19) are usually called the 'logarithmic wall functions' for the turbulent transport of momentum and heat, respectively. These expressions are only applicable for $30<y^+<130$ in the case of a wall jet or natural convection at the surface, see Fig. 2 for the range of Eq. (18) and Nizou [13] for the range of Eq. (19). Therefore, care must be exercised when using these functions for predicting room air movement.

Using Eq. (12) the expression for the wall heat flux can be written as:

$$q_w=\rho C_p(T_w-T)C_\mu^{1/4}k^{1/2}/\{\sigma_t[1/\kappa\ln(Ey^+)+C_h]\} \quad (21)$$

where $\sigma_t=0.9$ and $E=9.793$.

From Eqs. (12) and (13), the heat flux can be expressed as:

$$q_w=\frac{\rho u_\tau C_p(T_w-T_p)}{T^+} \quad (22)$$

where T_p is the fluid temperature at the first grid point from the wall.

The expression for the surface heat transfer coefficient, h, is given by:

$$q_w=h(T_w-T_{ref}) \quad (23)$$

where T_w is the temperature of the surface and T_{ref} is a reference temperature such as the bulk fluid temperature or the temperature at the edge of the thermal boundary layer.

An expression for h can be obtained by combining Eqs. (22) and (23), viz.:

$$h=\frac{\rho u_\tau C_p}{T^+}\left(\frac{T_w-T_p}{T_w-T_{ref}}\right) \quad (24)$$

2.4.2. Viscous sublayer region (low Reynolds number $k-\varepsilon$ model)

In the viscous sublayer region, where $\tau_l \gg \tau_t$, the heat transfer is predominately by conduction and the wall heat flux is given by:

$$q_w=-k\frac{\partial T}{\partial y}=-k\left(\frac{T-T_w}{y}\right) \quad (25)$$

Substituting Eq. (21) in Eq. (12) and re-arranging gives:

$$T^+=\sigma y^+ \quad (26)$$

Because the heat convected to the fluid is equal to that conducted from the surface, Eqs. (23) and (25) can be combined to give an expression for h as follows:

$$h=\frac{k}{y_p}\left[\frac{T_w-T_p}{T_w-T_{ref}}\right] \quad (27)$$

where k is the thermal conductivity of the fluid.

For Eq. (25) to be applicable, the transport equations must be solved up to the wall region, including the sublayer region. This requires a low Reynolds number turbulence model. In this paper, a 2D version of VORTEX [8] incorporating the low Reynolds number $k-\varepsilon$ model of Lam and Bremhost [7] is used. The choice of this model has been based on the work of Henkes and Hoogendroon [6]. Comparing the results from nine models, they found that this model produced accurate predictions of the heat transfer from a vertical plate up to a Grashof number of 10^{11} which is the maximum range used in this paper.

3. Experimental setup

The experimental results used here for comparison with the numerical predictions have been obtained from an extensive research programme using an environmental chamber and a test box. The chamber has external dimensions 4.00 m × 3.00 m × 2.5 m with two inner compartments: an environmental control compartment and a main chamber of dimensions 2.78 m × 2.78 m × 2.3 m (ceiling height), see Fig. 3. The environmental compartment is equipped with a cooling coil and a fan which is capable of cooling the compartment to −5°C and also heating it to 35°C if required. In this work the environmental compartment was the heat sink. In addition to this chamber a small box with internal dimensions 1.07 m × 1.01 m × 1.05 m high was required for other experiments to investigate the scale effect on the heat transfer coefficients. This box was constructed with an internal layer of 12 mm plywood covered by a 50 mm expanded polystyrene slab and then sealed with a polythene sheet.

Heating plates were attached to the inner surface of the chamber or the small box which was to be heated. These were constructed from a 2 mm sheet of polished aluminium, a Flexel sheet heating element (about 1 mm thick) and a 6 mm thick sheet of plywood. Holes of 6 mm were drilled into the aluminium for housing four-wire platinum resistance temperature (PRT) sensors (accuracy = ±0.15 K). Further details of the chamber, the heating plates and the measuring techniques can be found in Ref. [2].

To deduce the heat flux entering the chamber, Q_w, the conduction loss from the heated surface to the outside was first calculated using:

$$Q_w=P-\frac{kA}{L}(T_i-T_o) \quad (28)$$

where

$$Q_w=Q_r+Q_c \quad (29)$$

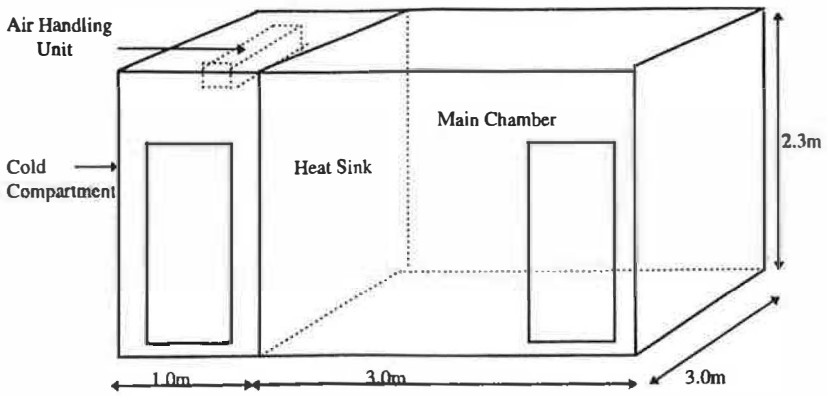

Fig. 3. The environmental chamber.

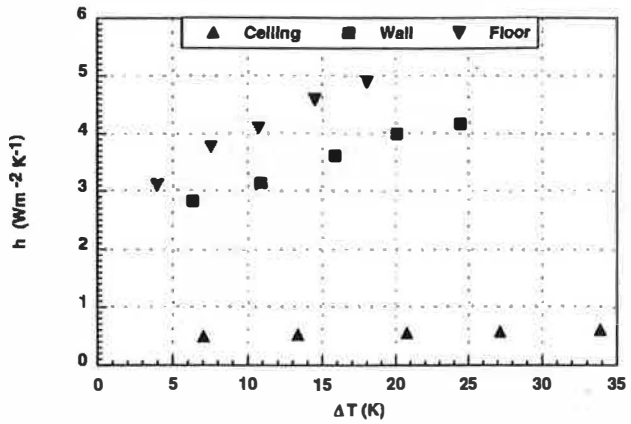

Fig. 4. Measured convective heat transfer coefficients for chamber surfaces.

The radiative heat flux is calculated using:

$$Q_r = \frac{A\varepsilon[\sigma T_i^4 - q_j]}{1-\varepsilon} \tag{30}$$

The convective heat transfer, Q_c, is obtained from Eq. (29) and h is calculated using:

$$h = \frac{Q_c}{A(T_w - T_{ref})} \tag{31}$$

A computer program ('CHTC') developed in FORTRAN incorporates the above equations to calculate the local and mean htc's. The calculations for the radiosity, q_j, were carried out by the same program by solving the radiation matrices and shape factors using the Gauss–Seidel method. For further details see Awbi and Gan [14].

4. Results and discussion

4.1. Experimental heat transfer coefficients

The surface heat transfer coefficients for the wall, floor and ceiling which were calculated from measurements in the large chamber, under natural convection, are shown in Fig. 4. The expressions given in Table 2 represent these values and the values obtained from measurements in the small box. The value of h for all the surfaces may be expressed by the formula:

$$h = \frac{C}{D^m}(\Delta T)^n \tag{32}$$

where C is a constant, D is the hydraulic diameter of the heated surface and m and n are indices. Using the single-sample error analysis method it was found that the predicted error in the measurement of h is dependent on the surface temperature with a *maximum* value of ± 0.4 W m^{-2} K for the wall, ± 0.6 W m^{-2} K for the floor and ± 0.1 W m^{-2} K for the ceiling. These results are valid for at least the range of temperature difference used in the experiments which is 5–35 K. The corresponding range of Grashof number is 9×10^8–1×10^{11}. The results have been obtained from tests in the two boxes described earlier which had a geometric ratio of about 2.7:1.

4.2. Heat transfer coefficients using wall functions

Eq. (24) has been used to calculate the convective heat transfer coefficient for a two dimensional cavity of the same dimensions as the large test chamber, i.e., 2.78 m wide and

Table 2
Natural convective heat transfer coefficients for heated room surfaces

Heated surface	Mean convective coefficient	Nusselt number	Range
Wall	$h=(1.823/D^{0.121})(\Delta T)^{0.293}$	$Nu=0.289(Gr)^{0.293}$	$9\times10^8<Gr<6\times10^{10}$
Floor	$h=(2.175/D^{0.076})(\Delta T)^{0.308}$	$Nu=0.269(Gr)^{0.308}$	$9\times10^8<Gr<7\times10^{10}$
Ceiling	$h=(0.704/D^{0.601})(\Delta T)^{0.133}$	$Nu=1.78(Gr)^{0.133}$	$9\times10^8<Gr<1\times10^{11}$

2.3 m high, using the CFD program VORTEX. The position of the first grid point was varied from 5 to 30 mm to determine the influence of y^+ on the value of h. The reference temperature, T_{ref}, in Eq. (24) was taken at the same locations as those used for determining h in the experiments, i.e., at 100 mm from the surface for the wall and floor. Beyond this distance, the air temperature for a heated wall or floor remained essentially constant. However, the location of T_{ref} for a heated ceiling was not as well defined, as can be seen from the measured temperature profile in Fig. 5. In this case, beyond a distance of 100 mm from the ceiling the air temperature does not remain constant but it continues to decrease, although at a much lower rate beyond about 1 m from the ceiling. As a result, T_{ref} for the ceiling was taken to be the air temperature at the centre of the chamber, i.e., at 1.15 m for the large chamber and 0.52 m for the small box. The same position for T_{ref} was also used in the CFD computations.

Different mesh sizes were used to establish grid-independency of the results and an optimum grid of 38×24 in the x- and y-direction, respectively was used for the calculations. The results which were obtained for the three room surfaces are shown in Fig. 6. This figure represents temperature difference ΔT for the wall, floor and ceiling of 24.4, 18.1 and 33.9 K, respectively.

The figure shows that the calculated heat transfer coefficient for all the room surfaces decreases as the distance y_p of the point at which T_p is specified increases. Similar results were also found by Nui and van der Kooi [5] for a window. By comparing the computed results with measurements it can be seen that the optimum distance for calculating h is about 5 mm from the surface for the wall and floor and about 30 mm from the ceiling.

The computed results show no variation of h with position on the wall and ceiling and only small variation for some of the floor results. The measured data, however, show some variation with position particularly for the wall and floor. The variation along the wall appear to coincide with transition from laminar to turbulent boundary layer at a height of about 0.7 m from the floor ($Gr \approx 1.5 \times 10^9$). On the other hand, the variation of h on the floor was caused by the downdraught from the cold sink which is to the left of the floor, i.e., 0 m.

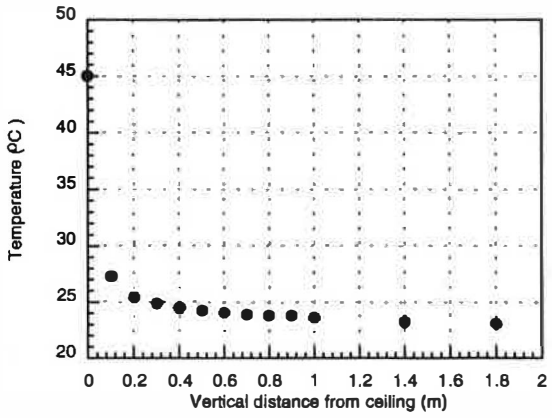

Fig. 5. Air temperature profile in the chamber for a heated ceiling.

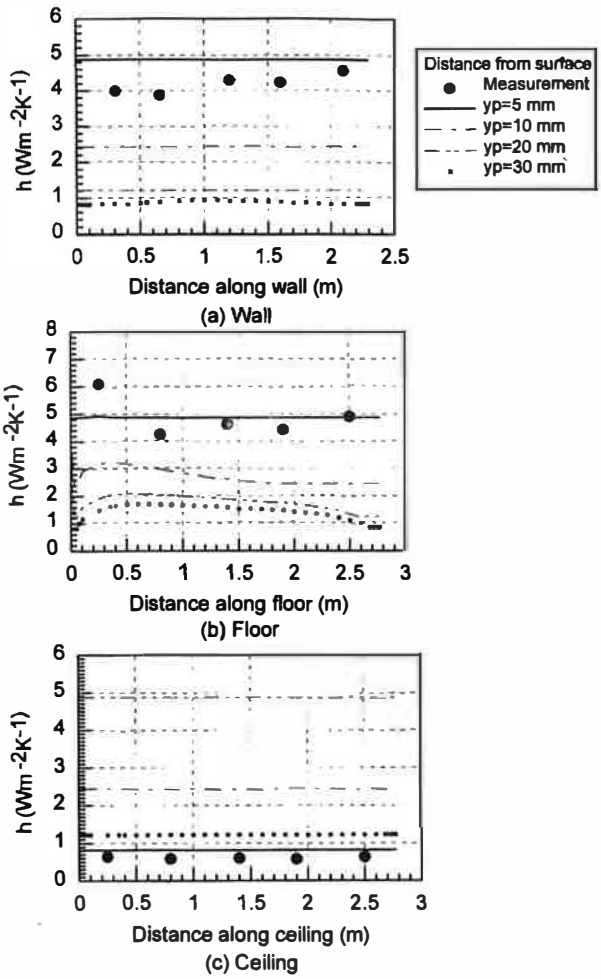

Fig. 6. Effect of distance from surface on h calculated using a wall function.

It is clear from these results that, in general, standard wall functions will not accurately predict the heat transfer from a room surface because the value of h is very sensitive to the distance from the surface at which the calculations are made. This may be due to the fact that most available wall functions are empirical expressions that have been based on data from forced convection in pipes and over isolated flat plates.

Schild [15] has carried an extensive study on the numerical prediction of heat transfer from room surfaces. He concluded that the standard wall functions are inadequate for modelling natural convection in rooms because the results are not independent of the near-wall grid resolution. He used the data given in Table 2 in both a zonal air flow model and a CFD model, each coupled with a building thermal model. He concludes that this alternative approach overcomes the uncertainty in applying standard wall functions in natural convection calculations.

4.3. Heat transfer coefficients using a low Reynolds number $k-\varepsilon$ model

The version of VORTEX with the low Reynolds number $k-\varepsilon$ model of Lam and Bremhost [7] was used to calculate

the local heat transfer coefficient for a two-dimensional cavity. Eq. (27) was used with T_{ref} taken at the same position from the surface as in the case of the wall function calculations. The position of the first grid point, y_p, hence y^+ was varied to investigate its effect on the calculated value of h. The range of y^+, corresponding to the values of y_p used, which was calculated at the centre of each heated surface was typically:

wall:	$y^+ = 1.5$–4.5
floor:	$y^+ = 0.7$–3.1
ceiling:	$y^+ = 0.02$–0.2

The grid size used in the computation was 125×125 and the distance of the first point from a surface was about 0.1 mm. Calculations were also made using grids ranging from 69×69 to 199×199 but there was little improvement in the predictions when a grid finer than 125×125 was used.

The results for the three room surfaces are shown in Fig. 7. These results show that the calculated value of h also increases slightly as y_p increases up to about $y_p = 1.0$ mm. For $y_p > 1.0$ mm, the increase in h is much larger. This would suggest that when $y_p > 1.0$ mm, the first grid point may, in some cases, be outside the laminar sublayer. However, the variation in h with y_p is, in this case, much smaller than that with the wall functions. Furthermore, the variation of h with position over the surface is predicted better here than in the previous case. The optimum distance, y_p, for calculating h in this case is about 0.5 mm from the surface.

It is clear from these results that if accurate calculations of the heat transfer from internal room surfaces are required for a CFD simulation then a low Reynolds number turbulence model will be needed. However, such models require a very large number of grid points to obtain an accurate solution which makes them less attractive for solving 3D problems. A more practical approach will be to use Eq. (32) to determine the natural convection from room surfaces. Eq. (32) can be incorporated in a CFD program or a zonal air flow model very readily as has been demonstrated by Schild [15]. Although this expression is based on tests carried out in two chambers, one representing a small room and the other a small box, the hydraulic diameter of the surface is included in the expression. Consequently this expression should apply to rooms of other sizes under natural convection providing that the Grashoff number is within the range of this study.

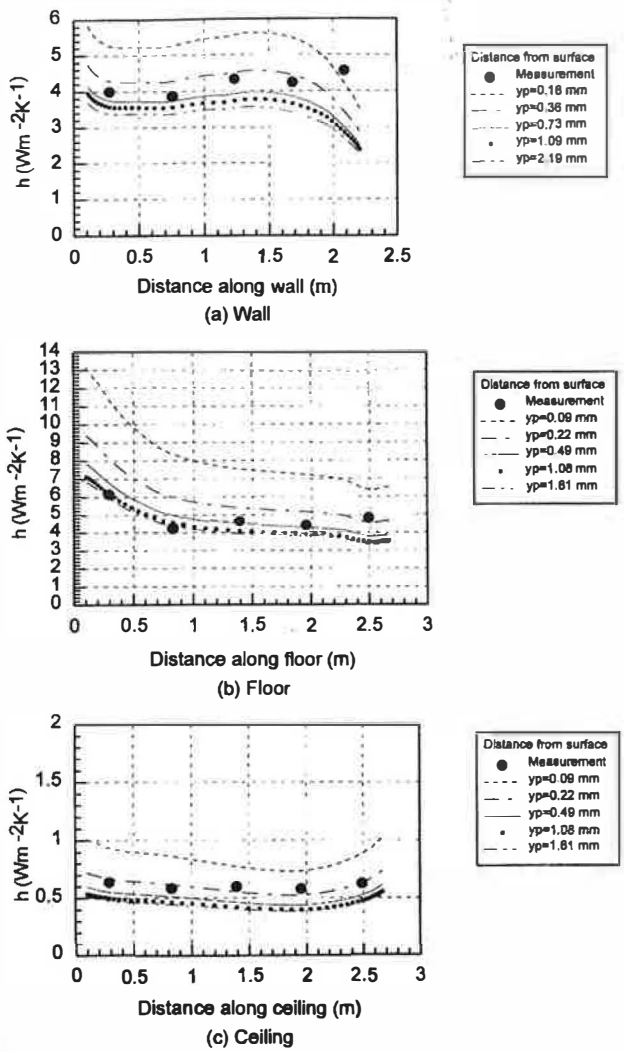

Fig. 7. Effect of distance from surface on h calculated using a low Reynolds number $k-\varepsilon$ model.

5. Conclusions

The results presented in this paper show that standard 'logarithmic wall functions', which are used in many CFD programs, do not produce an accurate representation of the heat transfer from internal room surfaces for natural convection heat transfer from these surfaces. The wall functions do not predict the variation of h over a heated surface of a room. Furthermore, the convective heat transfer coefficient predicted using a wall function is extremely sensitive to the distance of the point from the surface (y_p) at which the wall function is applied, i.e., the value of y^+ at that point. Although, in the present study, an optimum position of about 5 mm for a heated wall or a heated floor and about 30 mm for a heated ceiling were found, these values may not be universally valid and the optimum distance could well depend on the situation at hand as well as the type of wall function being used in the calculation.

As has previously been discovered by other investigators, a more accurate prediction of the heat transfer from room surfaces can be obtained using a low Reynolds number turbulence model. However, this type of model can be very expensive in computing terms for 3D problems and it is still mainly used for research purposes. A more plausible alternative will be to use, in a CFD or a zonal air flow code, experimentally determined expressions for h for room surfaces. This has been successfully demonstrated in a recent

study by Schild [15]. Such expressions are given in this paper as Eq. (32) which should be applicable to heated walls, floors and ceilings within the range of Grashof number that have been derived for. Unlike wall functions, Eq. (32) has been obtained for natural convection in enclosures.

6. Nomenclature

A	Area of heated surface (m^2)
A_{C1}, A_t, A_μ	Turbulence model constants
C, C_h	Constants
C_p	Specific heat ($J\,kg^{-1}\,K^{-1}$)
$C_\mu, C_{\varepsilon 1}, C_{\varepsilon 2}$	Turbulence model constants
D	Hydraulic diameter (m), turbulence model constant
E	Logarithmic constant, turbulence model constant
f	Function
f_1, f_2, f_μ	Turbulence model functions
h	Convective heat transfer coefficient ($W\,m^{-2}\,K$)
k	Kinetic energy of turbulence ($m^2\,s^{-2}$) or thermal conductivity ($W\,m^{-1}\,K^{-1}$)
L	Thickness (m)
P	Power input (W)
Q	Heat flux (W)
q_j	Radiosity ($W\,m^{-2}$)
q_w	Wall heat flux ($W\,m^{-2}$)
R_t, R_k	Turbulence Reynolds numbers
T	Temperature (°C)
T^+	Dimensionless temperature, $\rho C_p u_\tau (T_w - T_p)/q_w$
T_τ	Friction temperature, $q_w/(\rho C_p u_\tau)$
u, v, w	Velocity components ($m\,s^{-1}$)
u^+	Non-dimensional velocity, u/u_τ
u_τ	Friction velocity, $u_\tau = \sqrt{(\tau_w/\rho)}$
x, y, z	Cartesian coordinates
y^+	Local Reynolds number, $y^+ = u_\tau y/\nu$

Greek symbols

ε	Emissivity
κ	Karman's momentum constant ($\kappa = 0.4187$)
κ_h	Karman's heat transfer constant
μ	Absolute viscosity (Pa s)
ν	Kinematic viscosity ($m\,s^{-2}$)
ρ	Fluid density ($kg\,m^{-3}$)
σ	Laminar Prandtl/Schmidt number, or Stefan–Boltzmann constant ($\sigma = 5.67 \times 10^{-8}\ W\,m^{-2}\,K^{-4}$)
$\sigma_k, \sigma_t, \sigma_\varepsilon$	Prandtl number for turbulence energy, turbulent flow, and turbulence energy dissipation
τ	Shear stress (Pa)

Subscripts

a	Air
c	Convective
i	Inside surface
l	Laminar
o	Outside surface
p	Reference point or first iteration point from surface
r	Radiant
ref	Reference value
t	Turbulent
w	Wall
τ	Friction

Superscripts

-	Time mean value
'	Fluctuating value
+	Denotes dimensionless variable

Acknowledgements

This work was supported by the Engineering and Physical Sciences Research Council, UK, under grant reference GR/J47606. The assistance of Andrew Hatton and Stephen Tames in the experimental work is acknowledged.

References

[1] H. Eppel, K. Lomas, Empirical validation of three simulation programs using data from a passive solar building, Proc. of Building Simulation '95, August 14–16, Madison, WI, USA, 1995, pp. 588–595.
[2] A. Hatton, H.B. Awbi, Heat transfer from room surfaces, Proc. of ROOMVENT '96, Vol. 2, Yokohama, Japan, 1996, pp. 395–402.
[3] X. Yuan, A. Huber, A. Schaelin, P. Hachmann, A. Moser, New wall functions for the numerical simulation of air flow pattern in rooms, Proc. of Roomvent '92, Vol. 1, Aalborg, Denmark, 1992, pp. 75–91.
[4] G.P. Hammond, Profile analysis of heat/mass transfer across the plane wall-jet, Proc. of the 7th International Heat Transfer Conference, Vol. 3, Munich, 1982, pp. 349–355.
[5] J. Niu, J. van der Kooi, Grid optimization of $k-\varepsilon$ turbulence model simulation of natural convection in rooms, Proc. of Roomvent '92, Vol. 1, Aalborg, Denmark, 1992, pp. 207–223.
[6] R.A.W.M. Henkes, C.J. Hoogendoorn, Comparison of turbulence models for the natural convection boundary layer along a heated vertical plate, Int. J. Heat Mass Transfer 32 (1989) 157–169.
[7] C.K.G. Lam, K. Bremhost, A modified form of the $k-\varepsilon$ model for predicting wall turbulence, Trans. ASME, J. Fluids Eng. 103 (1981) 456–460.
[8] G. Gan, H.B. Awbi, Numerical simulation of the indoor environment, Building Environ. 29 (1994) 449–459.
[9] T. Cebeci, A.M.O. Smith, Analysis of Turbulent Boundary Layers, Academic Press, 1974.
[10] Q. Chen, Indoor Air Flow, Air Quality and Energy Consumption of Buildings, PhD Thesis, Delft University of Technology, Netherlands, 1988.

[11] Q. Chen, Construction of a low Reynolds number $k-\varepsilon$ model, Phoenics J. Comput. Fluid Dynamics 3 (1990) 288–329.
[12] C.L.V. Jayatilaka, The influence of Prandtl number and surface roughness on the resistance of the laminar sublayers to momentum and heat transfer, Prog. Heat Mass Transfer 1 (1969) 193–329.
[13] P.Y. Nizou, Heat and momentum transfer in a plane turbulent wall jet, Trans. ASME, J. Heat Transfer 103 (1981) 138–140.
[14] H.B. Awbi, G. Gan, Computational fluid dynamics in ventilation, Proc. of CFD for Environmental and Building Services Engineer, Institution of Mechanical Engineers, London, 1991, pp. 67–79.
[15] P. Schild, Accurate Prediction of Indoor Climate in Glazed Enclosures, PhD Dissertation, Norwegian University of Science and Technology, Trondheim, Norway, 1997.